IMECE2002-34239

THE EFFECT OF DEFECTS AND ACOUSTIC IMPEDANCE MISMATCH ON HEAT CONDUCTION SIGE BASED SUPERLATTICES

Scott T. Huxtable
Department of Mechanical Engineering
University of California – Berkeley
Berkeley, CA 94720

Alexis R. Abramson
Department of Mechanical Engineering
University of California – Berkeley
Berkeley, CA 94720

Arun Majumdar
Department of Mechanical Engineering
University of California – Berkeley
Berkeley, CA 94720

Ali Shakouri
Jack Baskin School of Engineering
University of California – Santa Cruz
Santa Cruz, CA 95064

Edward T. Croke
HRL Laboratories, LLC
Malibu, CA 90265

ABSTRACT

The cross-plane thermal conductivity of four Si/Ge, Si/Si$_{0.4}$Ge$_{0.6}$, and Si$_{0.9}$Ge$_{0.1}$/Si$_{0.1}$Ge$_{0.9}$ superlattices was measured using the 3ω technique. All four superlattices were found to have thermal conductivity values between 1.8 and 3.5 W/m-K, which are below the values of typical Si$_x$Ge$_{1-x}$ alloys. The growth quality of these superlattices was evaluated qualitatively through the use of x-ray diffraction and transmission electron microscopy. These studies indicated that the superlattices contained a relatively high density of defects. The low thermal conductivity values are presumed to be due in large part to these defects.

INTRODUCTION

The thermal conductivity of semiconductor superlattices is an important parameter for the performance of thermoelectric devices. Recently, numerous studies have reported thermal conductivity of several superlattice systems including GaAs/AlAs,[1-5] Si/Ge,[6,7] Si/Si$_x$Ge$_{1-x}$ (Refs. 8 and 9), Si$_x$Ge$_{1-x}$/Si$_y$Ge$_{1-y}$ (Ref. 9), and Bi$_2$Te$_3$/Sb$_2$Te$_3$ (Refs. and). In several cases the thermal conductivity of the superlattice was found to be below the value of a comparable alloy of the same materials. While this reduction in thermal conductivity has been attributed to a variety of mechanisms including defect scattering, mini-bandgap formation, and interface scattering due to mismatches in phonon spectra and acoustic impedance, the specific reasons remain unclear. One major deficiency in much of the previous work is that there has been little effort to correlate the quality of the growth of the superlattices with the thermal conductivity data. Without knowledge of the quality of the interfaces, it is difficult to determine the relative importance of the various mechanisms in light of the potential presence of defects. This is particularly important in the growth of lattice mismatched systems, such as Si and Ge, where one could expect a significant number of defects in the growth of the superlattices.

DISCUSSION

Recently, we measured the cross-plane thermal conductivity of several Si/Si$_{0.7}$Ge$_{0.3}$ superlattices (see Fig. 1) and found that the thermal conductivity decreased for decreasing period thickness (increasing number of interfaces).[9] For these four samples, the additional interfaces seemingly added a corresponding thermal boundary resistance. One possible cause for the thermal resistance associated with the interfaces could be the acoustic impedance mismatch between the two materials. Acoustic impedance is defined as the product of the mass density and the speed of sound (phonon group velocity) within the material. While the speed of sound is different for phonons of different frequency traveling in various crystal directions, an "average" acoustic impedance mismatch (AIM)
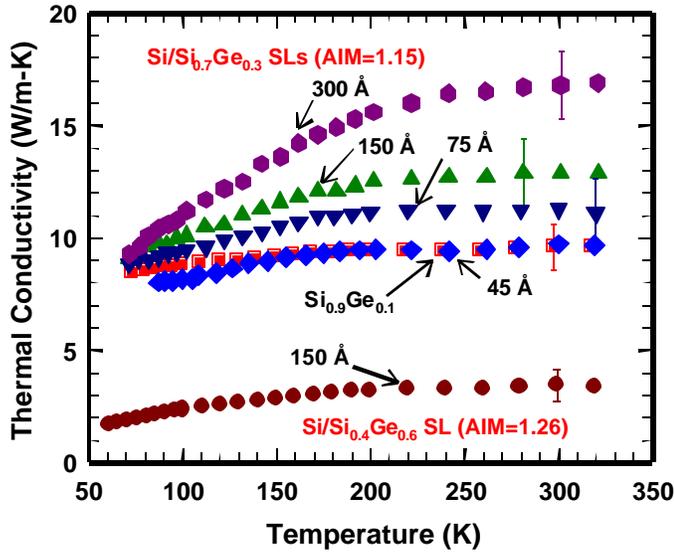
Fig. 1 Cross-plane thermal conductivity of four $Si/Si_{0.7}Ge_{0.3}$ superlattices, a 3.5 μm thick $Si_{0.9}Ge_{0.1}$ film, and a $Si/Si_{0.4}Ge_{0.6}$ superlattice. The label on each data set refers to the period thickness.
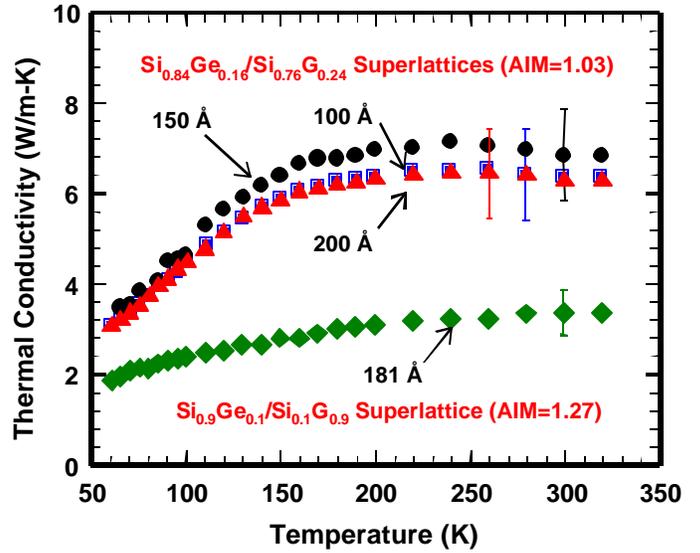

Fig. 2 Cross-plane thermal conductivity of three $Si_{0.84}Ge_{0.16}/Si_{0.76}Ge_{0.24}$ superlattices and a $Si_{0.9}Ge_{0.1}/Si_{0.1}Ge_{0.9}$ superlattice. The label on each data set refers to the period thickness.

for these superlattices was estimated to be ~1.15 by using a weighted average of the material properties for Si and Ge and averaging over the [100], [110], and [111] directions.

In the same study,[9] the cross-plane thermal conductivity of three $Si_{0.84}Ge_{0.16}/Si_{0.76}Ge_{0.24}$ superlattices was found to be essentially independent of period thickness for periods between 100 Å and 200 Å (see Fig. 2). Given that the alloy composition of each layer was quite similar, the estimated AIM of these samples was only ~1.03. Since the AIM was so low, the interfaces did not play a significant role with regard to heat conduction and alloy scattering was dominant.

In attempt to find a Si_xGe_{1-x} based superlattice with a thermal conductivity below the alloy limit, we then grew four new superlattices with higher acoustic impedance mismatches. Two were Si/Ge (AIM ~1.37), the third sample was $Si/Si_{0.4}Ge_{0.6}$ (AIM ~1.26) and the final one was $Si_{0.9}Ge_{0.1}/Si_{0.1}Ge_{0.9}$ (AIM ~1.27). These samples were grown by molecular beam epitaxy (MBE) at HRL Laboratories, LLC. The Si/Ge superlattices were grown on buffer layers that consisted of a 1 μm thick film of $Si_{0.8}Ge_{0.2}$ followed by a 1 μm thick $Si_{0.8}Ge_{0.2}/Si_{0.745}Ge_{0.25}C_{0.005}$ superlattice. One Si/Ge superlattice had a period thickness of 50 Å (40 Å Si, 10 Å Ge) and a total thickness of 1.35 μm, while the other sample had a period thickness of 60 Å (30 Å Si, 30 Å Ge) and a total thickness of 3 μm. Both samples were doped with boron concentrations of ~5 × 10^{19} cm^{-3}, and had 0.3 μm thick capping layers of $Si_{0.8}Ge_{0.2}$. The other two superlattices were each 0.5 μm thick and were grown on 1 μm thick Si_xGe_{1-x} buffer layers that were relaxed to the lattice constant of $Si_{0.8}Ge_{0.2}$. The $Si/Si_{0.4}Ge_{0.6}$ superlattice had a period of 150 Å (100 Å Si, 50 Å

$Si_{0.4}Ge_{0.6}$) and was doped with a boron concentration of ~6 × 10^{19} cm^{-3}, while the $Si_{0.9}Ge_{0.1}/Si_{0.1}Ge_{0.9}$ sample had a period of 181 Å (23 Å $Si_{0.1}Ge_{0.9}$, 158 Å $Si_{0.9}Ge_{0.1}$) and a boron concentration of ~1.5 × 10^{20} cm^{-3}.

The cross-plane thermal conductivity was then measured using the 3ω method.[12,13] This technique utilizes a thin metal line that is patterned on the surface of the sample as both an electrical resistance heater and a thermometer. Since these superlattice samples are electrically conducting, a thin (~100 – 150 nm thick) SiO_2 layer was first deposited on the surface of the sample in order to provide insulation between the heater/thermometer line and the sample. This technique measures the total thermal resistance of the superlattice along with the buffer, cap, and oxide layers. Therefore, the contribution of these extra layers must be measured separately and subtracted out from the raw data. In order for the cross-plane thermal conductivity to be measured directly, the ratio of the width of the heater/thermometer line to the thickness of the sample must be large such that the heat flow through the superlattice may be assumed to be one-dimensional. The validity of this assumption and errors associated with it will be briefly discussed later.

Figure 1 shows the measured thermal conductivity of the $Si/Si_{0.4}Ge_{0.6}$ superlattice in comparison with the $Si/Si_{0.7}Ge_{0.3}$ samples measured previously. The thermal conductivity of the $Si/Si_{0.4}Ge_{0.6}$ sample was found to be ~60% less than the lowest thermal conductivity measured for the $Si/Si_{0.7}Ge_{0.3}$ samples at room temperature and ~70% less than the value measured for the $Si/Si_{0.7}Ge_{0.3}$ sample with the same period thickness. Similarly,
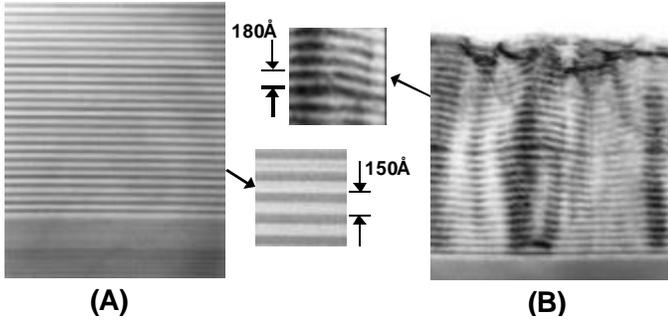
Fig. 3 Transmission electron microscopy (TEM) images of two superlattice cross-sections. (A) $Si_{0.76}Ge_{0.24}/Si_{0.84}Ge_{0.16}$ superlattice with high quality interfaces. (B) $Si_{0.9}Ge_{01}/Si_{0.1}Ge_{0.9}$ superlattice with defects. The mismatch in lattice parameters of the two layers in (A) is only ~0.3%, while in (B) it is ~3.1%, which leads to higher strain and, ultimately, many defects.

the thermal conductivity of the $Si_{0.9}Ge_{0.1}/Si_{0.1}Ge_{0.9}$ superlattice was found to be ~50% less than the value measured for the $Si_{0.84}Ge_{0.16}/Si_{0.76}Ge_{0.24}$ superlattices, as shown in Fig. 2. Additionally, the thermal conductivity of this superlattice fell below that of Si_xGe_{1-x} alloys at room temperature, as published reports on the thermal conductivity of Si_xGe_{1-x} alloys indicate a minimum value of ~4 – 5 W/m-K regardless of the Ge content or doping level.[14,15]

There are several possible explanations for these low thermal conductivity values. The first item that should be addressed is experimental error. While the reliability of the experimental setup has been verified in the past for substrates and thin oxide films, it should be noted that the superlattices measured previously (the $Si/Si_{0.7}Ge_{0.3}$ and $Si_{0.84}Ge_{0.16}/Si_{0.76}Ge_{0.24}$ samples) were all 3 μm thick while the current samples are only 0.5 μm thick. Since the heater/thermometer lines were all approximately the same width (~25 μm) the validity of the one-dimensional heat flow assumption must be assessed. Borca-Tasciuc *et al.*[16] recently quantified the amount of error that could be expected for a given geometry and sample anisotropy. Using their analysis, the error associated with the one-dimensional assumption for the 0.5 μm thick superlattices should be less than a few percent. However, the reported thermal conductivities of the previous 3 μm thick samples may have been overestimated by up to ~25%. Therefore, errors associated with the one-dimensional assumption on the previous samples could account for some, but certainly not nearly all, of the observed reduction in thermal conductivity. A second possibility is that the difference in the thermal conductivity of the individual alloy layers could contribute to the reduced thermal conductivity of the superlattice structure. The difference in thermal conductivity of $Si_{0.7}Ge_{0.3}$ and $Si_{0.4}Ge_{0.6}$ was shown to be less than 10% (Ref. 15), therefore any difference between the measured thermal conductivity of the $Si/Si_{0.4}Ge_{0.6}$ sample and the previous $Si/Si_{0.7}Ge_{0.3}$ superlattices is expected to be due to different conditions at the interface.
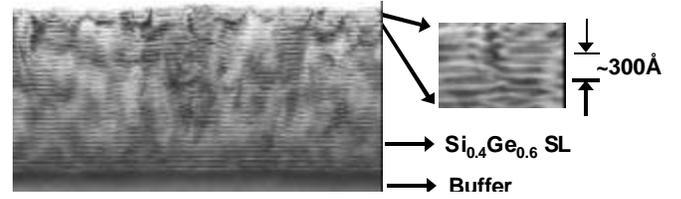

Fig. 4 TEM image of the $Si/Si_{0.4}Ge_{0.6}$ superlattice. This image shows significant defects throughout the structure, particularly when compared with Fig. 4.7. The defect density increases with the overall thickness of the structure as the strain in each layer increases until it is relieved through the formation of defects.

Similarly, the $Si_{0.9}Ge_{0.1}$ layer in the $Si_{0.9}Ge_{0.1}/Si_{0.1}Ge_{0.9}$ superlattice should have a thermal conductivity value close to both $Si_{0.84}Ge_{0.16}$ and $Si_{0.76}Ge_{0.24}$, while the conductivity of $Si_{0.1}Ge_{0.9}$ should actually be *higher* than either of the two previous layers.[15]

Another potential physical mechanism for this observed reduction is the increased acoustic impedance mismatch that was designed into these samples. While it is tempting to initially attribute the low thermal conductivity solely to this mechanism it is important to note that as the alloy compositions were changed to increase the AIM, the lattice parameters also were affected. As the mismatch in lattice constants increased,

Sample Description	Period (Å)	FWHM (deg)
$Si/Si_{0.7}Ge_{0.3}$	45	0.0352
$Si/Si_{0.7}Ge_{0.3}$	75	0.0359
$Si/Si_{0.7}Ge_{0.3}$	150	0.0300
$Si/Si_{0.7}Ge_{0.3}$	300	0.0282
$Si_{0.84}Ge_{0.16}/Si_{0.74}Ge_{0.26}$	100	0.0577
$Si_{0.84}Ge_{0.16}/Si_{0.74}Ge_{0.26}$	150	0.0606
$Si_{0.84}Ge_{0.16}/Si_{0.74}Ge_{0.26}$	200	0.0650
$Si/Si_{0.6}Ge_{0.4}$	150	0.1116
$Si_{0.9}Ge_{0.1}/Si_{0.1}Ge_{0.9}$	181	No peak
Si/Ge	50	0.1856
Si/Ge	60	No peak

Table 1 FWHM of xray diffraction rocking curve data on superlattices. The larger FWHM values (above ~0.1) indicate poor superlattice growth quality.

the chance of defects being introduced during the growth process also increased. For example, the original $Si/Si_{0.7}Ge_{0.3}$ superlattices had an AIM of ~1.15 and a lattice mismatch of ~1.3%. The $Si/Si_{0.4}Ge_{0.6}$ sample had an increased AIM of ~1.26, but the lattice mismatch also rose to ~2.5%. Similarly, the $Si_{0.9}Ge_{0.1}/Si_{0.1}Ge_{0.9}$ sample had an AIM of ~1.27 and a lattice mismatch of ~3.3%, compared to values of ~1.03 and ~0.4% for the $Si_{0.84}Ge_{0.16}/Si_{0.76}Ge_{0.24}$ superlattices. Since the lattice mismatch of both samples increased dramatically, the quality of the crystal growth should be examined in order to determine if defects may have been introduced in the samples.

Accurately quantifying the defect density in a superlattice is a difficult task. However, the general growth quality can be assessed qualitatively through the use of cross-sectional transmission electron microscopy (TEM) and/or x-ray diffraction[17] (XRD). Figure 3 shows TEM images of the $Si_{0.84}Ge_{0.16}/Si_{0.76}Ge_{0.24}$ and $Si_{0.9}Ge_{0.1}/Si_{0.1}Ge_{0.9}$ superlattices. Clearly, the $Si_{0.9}Ge_{0.1}/Si_{0.1}Ge_{0.9}$ sample is not of the same quality as the first alloy/alloy superlattice. The initial layers were relatively smooth, but as the strain built up, the interfaces began to undulate and defects were created. The $Si/Si_{0.4}Ge_{0.6}$ superlattice is shown in Fig. 4 and it also contains a high density of defects. With TEM images of several samples a reference, XRD can be used to quickly examine the quality of other similar superlattices. Atomically abrupt interfaces will give sharp peaks in the x-ray data, while rougher interfaces will have broader peaks. By comparing the full width at half maximum (FWHM) of the intensity peaks of similarly composed superlattices one can get a relative idea of the amount of defects at the interfaces. Table 1 shows FWHM data for all of the superlattices in this study along with the four $Si/Si_{0.7}Ge_{0.3}$ superlattices measured previously. Based on these data it seems reasonable to assume that the $Si/Si_{0.7}Ge_{0.3}$ samples were of high quality due to the fact that their peaks were even sharper than those of the $Si_{0.84}Ge_{0.16}/Si_{0.76}Ge_{0.24}$ superlattices. The XRD data also confirmed the poor growth of the $Si/Si_{0.4}Ge_{0.6}$ and $Si_{0.9}Ge_{0.1}/Si_{0.1}Ge_{0.9}$ superlattices. Finally, the XRD data indicated that the two Si/Ge superlattices were of poor quality as well.

The thermal conductivity of the two Si/Ge superlattices is shown in Fig. 5 along with data on a Si/Ge superlattice from Lee *et al.*[6] and the previously discussed data for the $Si_{0.9}Ge_{0.1}/Si_{0.1}Ge_{0.9}$ and $Si/Si_{0.4}Ge_{0.6}$ samples. The thermal conductivity for the two Si/Ge samples was below that of the previous samples, which is understandable given the fact that the lattice mismatch and AIM are greater for Si/Ge.

The reason that the Si/Ge sample with the 60 Å period had a lower thermal conductivity is believed to be due to the fact that it had more defects. Although the period thickness was only slightly larger, the 60 Å sample was 3 μm thick, while the 50 Å sample was only 1.35 μm thick. This increased thickness leads to more strain and more defects. The XRD data confirmed the fact that the 60 Å sample was of lower quality.

The discrepancy between the 50 Å sample reported here and the data from Lee *et al.*[6] is likely due to the different growth conditions and techniques for the samples. Their samples were grown by metalorganic chemical vapor deposition (MOCVD) at 750 °C, while these samples were grown by MBE at ~500 °C.

SUMMARY

The 3ω technique was used to measure the cross-plane thermal conductivity of four Si/Ge, $Si/Si_{0.4}Ge_{0.6}$, and $Si_{0.9}Ge_{0.1}/Si_{0.1}Ge_{0.9}$ superlattices. These samples were examined in comparison with several $Si/Si_{0.7}Ge_{0.3}$ and $Si_{0.84}Ge_{0.16}/Si_{0.76}Ge_{0.24}$ superlattices that were measured previously. The current samples were found to possess thermal conductivities considerably lower than the earlier samples. Furthermore, their thermal conductivities were below values that are typical of Si_xGe_{1-x} alloys and approached values associated with amorphous materials.

These superlattices were designed to have an increased acoustic impedance mismatch in comparison with the samples measured previously. However, along with the increase in acoustic impedance, there was a corresponding increase in lattice mismatch. It was shown through the use of x-ray diffraction and transmission electron microscopy that this increased lattice mismatch led to the creation of a large density of defects within the superlattices. Since the defects are expected to scatter phonons strongly and are believed to be largely responsible for the observed reduction in thermal conductivity, it was not possible conclusively determine the significance of the increased acoustic impedance mismatch.
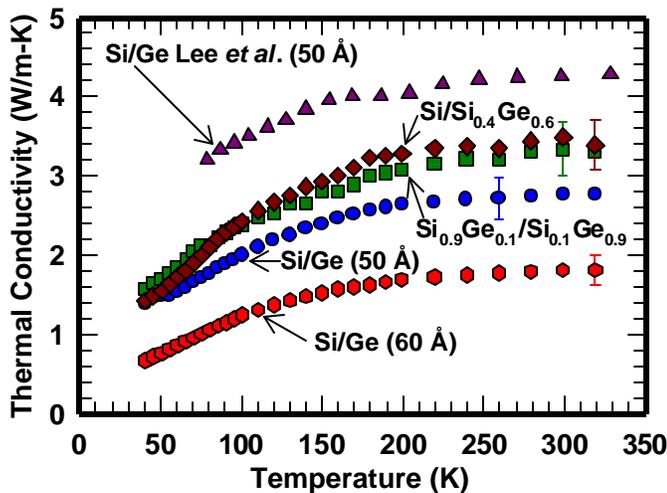

Fig. 5 Cross-plane thermal conductivity of Si/Ge superlattices. The two lowest data sets are for Si/Ge superlattices with periods of 50 Å (40 Å of Si and 10 Å of Ge) and 60 Å (30Å of Si and 30 Å of Ge), respectively. The next two sets of data are for the $Si/Si_{0.4}Ge_{0.6}$ and $Si_{0.9}Ge_{0.1}/Si_{0.1}Ge_{0.9}$ superlattices that were measured previously and are plotted here for comparison. The upper data set is for a Si/Ge superlattice with a period of 50 Å (~36 Å of Si and ~14 Å of Ge) from Lee *et al.*[6]

Copyright © 2002 by ASME

Work is currently underway to optimize the growth conditions such that defect-free Si_xGe_{1-x} based superlattices with higher AIM values can be fabricated.

ACKNOWLEDGMENTS

REFERENCES

1   Yao, T., "Thermal properties of AlAs/GaAs superlattices," *Applied Physics Letters*, Vol. 51, pp. 1798 – 1800, 1987.

2   Capinski, W. S., and Maris, H. J., "Thermal conductivity of GaAs/AlAs superlattices," *Physica B*, Vol. 219 & 220, pp. 699 – 701, 1996.

3   Capinski, W. S., Maris, H. J., Ruf, T., Cardona, M., Ploog, K., and Katzer, D. S., "Thermal-conductivity measurements of GaAs/AlAs superlattices using a picosecond optical pump-and-probe technique," *Physical Review B*, Vol. 59, pp. 8105 – 8113, 1999.

4   Chen, G., Tien, C.-L., Wu, X., and Smith, J. S., "Thermal diffusivity measurement of GaAs/AlGaAs thin-film structures," *Journal of Heat Transfer*, Vol. 116, pp. 325 – 331, 1994.

5   Yu, X. Y., Chen, G., Verma, A., and Smith, J. S., "Temperature dependence of thermophysical properties of GaAs/AlAs periodic structure," *Applied Physics Letters*, Vol. 67, pp. 3554 – 3556, 1995.

6   Lee, S.-M., Cahill, D. G., and Venkatasubramanian, R., "Thermal conductivity of Si-Ge superlattices," *Applied Physics Letters*, Vol. 70, pp. 2957 – 2959, 1997.

7   Borca-Tasciuc, T., Liu, W., Liu, J., Zeng, T., Song, D. W., Moore, C. D., Chen, G., Wang, K. L., Goorsky, M. S., Radetic, T., Gronsky, R., Koga, T., and Dresselhaus, M. S., "Thermal conductivity of symmetrically strained Si/Ge superlattices," *Superlattices and Microstructures*, Vol. 28, pp. 199 – 206, 2000.

8   Chen, G., Zhou, S. Q., Yao, D.-Y., Kim, C. J., Zheng, X. Y., Liu, Z. L., and Wang, K. L., "Heat conduction in alloy-based superlattices," *17th International Conference on Thermoelectrics*, pp. 202 – 205, 1998.

9   S. T. Huxtable, A. R. Abramson, C.-L. Tien, A. Majumdar C. LaBounty, X. Fan, G. Zeng, and J. E. Bowers, "Thermal conductivity of Si/SiGe and SiGe/SiGe superlattices," *Applied Physics Letters*, Vol. 80, 1737 – 1739, 2002.

10 Venkatasubramanian, R., "Lattice thermal conductivity reduction and phonon localizationlike behavior in superlattice structures," *Physical Review B*, Vol. 61, pp. 3091 – 3097, 2000.

11 Touzelbaev, M. N., Zhou, P., Venkatasubramanian, R., and Goodson, K., "Thermal characterization of Bi Te /Sb Te superlattices," *Journal of Applied Physics*, Vol. 90, pp. 763 – 767, 2001.

12 Cahill, D. G., "Thermal conductivity measurement from 30 to 750 K: the 3 omega method," *Review of Scientific Instruments*, Vol. 61, pp. 802 – 808, 1990.

13 Cahill, D. G., Katiyar, M., and Abelson, J. R., "Thermal conductivity of a-Si:H thin films," *Physical Review B*, Vol. 50, pp. 6077 – 6081, 1994.

14 Steigmeier, E. F., and Abeles, B., "Scattering of phonons by electrons in germanium-silicon alloys," *Physical Review*, Vol. 136, pp. A1149 – A1155, 1964.

15 Dismukes, J. P., Ekstrom, L., Steigmeier, E. F., Kudman, I., and Beers, D. S., "Thermal and electrical properties of heavily doped Ge – Si alloys up to 1300°K," *Journal of Applied Physics*, Vol. 35, pp. 2899 – 2907, 1964.

16 Borca-Tasciuc, T., Kumar, A. R., and Chen, G., "Data reduction in 3ω method for thin-film thermal conductivity determination," *Review of Scientific Instruments*, Vol. 72, pp. 2139 – 2147, 2001.

17 Herman, M. A., and Sitter, H., Molecular Beam Epitaxy: Fundamentals and Current Status, Springer-Verlag, Berlin, 1989.